

Harmine Hydrochloride Triggers G2/M Cell Cycle Arrest and Apoptosis in HCT116 Cells through ERK and PI3K/AKT/mTOR Signaling Pathways

Gi Dae Kim

Department of Food and Nutrition, Kyungnam University, Gyeongnam 51767, Korea

ABSTRACT: Colorectal carcinoma (CRC) is one of the most common and aggressive malignant carcinomas. There is a pressing need to develop naturally derived novel drugs with minimal side effects for treatment of CRC. In this study, we aimed to investigate the anticancer effects of harmine hydrochloride (HMH), a hydrophilic and stable substance that is easily absorbed by tissues and similar to harmine, and the underlying mechanism of action in human CRC HCT116 cells. HMH inhibited the growth, colony formation, and migration ability of HCT116 cells. Additionally, HMH induced G2 cell cycle arrest by reducing expression of p-cdc2, cdc2, and cyclin B1, proteins that regulate the G2/M phase, and expression of Rb, a protein that regulates cell proliferation, in a dose-dependent manner. HMH mediated apoptosis by downregulating expression of apoptotic proteins (such as caspase-3, caspase-9, and PARP) and the anti-apoptotic protein Bcl-2 and by inducing expression of Bax, a pro-apoptotic protein. Furthermore, HMH reduced the levels of p-ERK, p-PI3K, p-AKT, and p-mTOR in HCT116 cells, and significantly inhibited p-ERK and p-AKT expression in cells treated with of HMH and PD98059, an ERK inhibitor, or LY294002, an AKT inhibitor ($P < 0.05$ and $P < 0.01$). These results demonstrate the inhibitory effect of HMH on cell proliferation and migration through inducing apoptosis by inhibiting ERK and PI3K/AKT/mTOR signaling pathways, indicating its potential therapeutic applications in CRC.

Keywords: apoptosis, ERK, G2/M, harmine hydrochloride, PI3K/AKT/mTOR

INTRODUCTION

Colorectal cancer (CRC) is one of the most common and aggressive malignant carcinomas (Torre et al., 2015). CRC is commonly treated by surgery or chemotherapy; however, chemotherapy is often ineffective and is associated with several side effects (Kuebler et al., 2007). Therefore, it is imperative to explore new approaches for treatment of CRC, including novel drugs derived from natural products that have minimal side effects.

Mitogen-activated protein kinases (MAPKs) regulate various cellular activities, such as cell proliferation, differentiation, migration, apoptosis, survival, inflammation, and innate immunity (Turjanski et al., 2007; Peti and Page, 2013). MAPKs, including c-Jun NH₂-terminal kinase (JNK), p38 MAPK, and extracellular signal-regulated kinase (ERK), are serine-threonine protein kinases. The JNK and p38 MAPK signaling pathways are activated by various types of cellular stress such as oxidative stress, differentiation, apoptosis, genotoxicity, and osmotic stress,

and microbial components such as bacterial lipopolysaccharides and inflammatory cytokines including tumor necrosis factor- α and interleukin-1 β (Arthur and Ley, 2013; Sabio and Davis, 2014). The ERK signaling pathway plays a central role in cancer cell proliferation and metastatic progression (Das Thakur and Stuart, 2014).

The phosphoinositide 3-kinase (PI3K)/protein kinase B (AKT)/mammalian target of rapamycin (mTOR) pathway is involved in regulation of physiological processes such as cell proliferation, growth, survival, adhesion, motility, migration, metabolism, and angiogenesis. The pathway is also involved in various pathological processes, such as metastasis and the development of colorectal (Papadatos-Pastos et al., 2015), breast (Qin et al., 2018), liver (Golob-Schwarzl et al., 2007), and pancreatic cancers (Murthy et al., 2018). Hyperactivation of the PI3K/AKT/mTOR signaling pathway has been reported in CRC (Kang et al., 2017). Therefore, metastasis, drug resistance, and cancer stemness, which mark the start of cancer, and the PI3K/AKT/mTOR pathway are potential targets for CRC treat-

Received 26 August 2021; Revised 28 September 2021; Accepted 30 September 2021; Published online 31 December 2021

Correspondence to Gi Dae Kim, Tel: +82-55-249-2176, E-mail: gidaekim@kyungnam.ac.kr
Author information: Gi Dae Kim (Professor)

Copyright © 2021 by The Korean Society of Food Science and Nutrition.

© This is an Open Access article distributed under the terms of the Creative Commons Attribution Non-Commercial License (<http://creativecommons.org/licenses/by-nc/4.0>) which permits unrestricted non-commercial use, distribution, and reproduction in any medium, provided the original work is properly cited.

ment (Bahrami et al., 2018).

Natural products have drawn the attention of researchers for several decades because of their anticancer properties (Mukherjee et al., 2001; McChesney, 2002). Harmine [7-methoxy-1-methyl-9H-pyrido(3,4-b)indole] is a β -carboline alkaloid extracted from the seeds of *Peganum harmala* L., a herbal plant that grows in dry regions such as the Middle East and certain regions in China. These seeds have been widely used in home remedies due to their anti-inflammatory and antitumor activities (Newman and Cragg, 2016). While harmine has remarkable pharmacological properties, its use has been considerably restricted owing to its low bioavailability and side effects. Although research is being conducted on harmine hydrochloride (HMH) (Liu et al., 2013; Zhang et al., 2016), studies on the mechanism of action of stable, anticancer HMH in CRC are lacking.

In the present study, we investigated the anticancer effects and mechanism of action of HMH, which is hydrophilic, stable, and easily absorbed by tissues. HMH exhibits the same characteristics as harmine in human CRC HCT116 cells (Zhang et al., 2020). We observed that HMH inhibits the growth of HCT116 cells by suppressing ERK and PI3K/AKT/mTOR pathways, consequently inducing cell cycle arrest and apoptosis.

MATERIALS AND METHODS

Materials

HMH (Fig. 1A; Sigma-Aldrich Co., St. Louis, MO, USA) was dissolved in 100% dimethyl sulfoxide (DMSO). A 50 mmol/L stock solution of HMH was prepared and stored

as small aliquots at -20°C until needed. DMSO, 3-(4,5-dimethylthiazol-2-yl)-2,5-diphenyltetrazolium bromide (MTT), and horseradish peroxidase (HRP)-conjugated anti-rabbit and anti-mouse antibodies were purchased from Sigma-Aldrich, an apoptosis detection kit was purchased from BD Biosciences (Franklin Lakes, NJ, USA), and 2,7-dichlorofluorescein (DCF) diacetate (H_2DCFDA) was purchased from Molecular Probes (Invitrogen, Carlsbad, CA, USA). Phospho-specific anti-JNK, anti-p38, anti-ERK, anti-PI3K, anti-AKT, and anti-mTOR antibodies, anti-caspase-3, anti-caspase-9, anti-poly(ADP-ribose) polymerase (PARP), anti-Bax, anti-Bcl-2, anti-JNK, anti-p38, anti-ERK, anti-PI3K, anti-AKT, and anti-mTOR specific antibodies, the ERK inhibitor PD98059, and the AKT inhibitor LY294002 were purchased from Cell Signaling Technology (Danvers, MA, USA). HRP-conjugated β -actin, p53, p21, p-cdc2, cdc2, cyclin B1, and Rb antibodies were purchased from Santa Cruz Biotechnology (Santa Cruz, CA, USA).

Cell culture

HCT116 human CRC cells were purchased from the American Type Culture Collection (Rockville, MD, USA) and cultured in Roswell Park Memorial Institute (RPMI)-1640 medium containing 10% fetal bovine serum (FBS) and 1% antibiotics-antimycotics at 37°C in a 5% CO_2 incubator.

Cell viability analysis

MTT assays were used to measure the viability of HCT116 cells following treatment with HMH. HCT116 cells (5×10^3 cells/mL) were seeded into 96-well plates and incubated overnight. The medium was subsequently re-

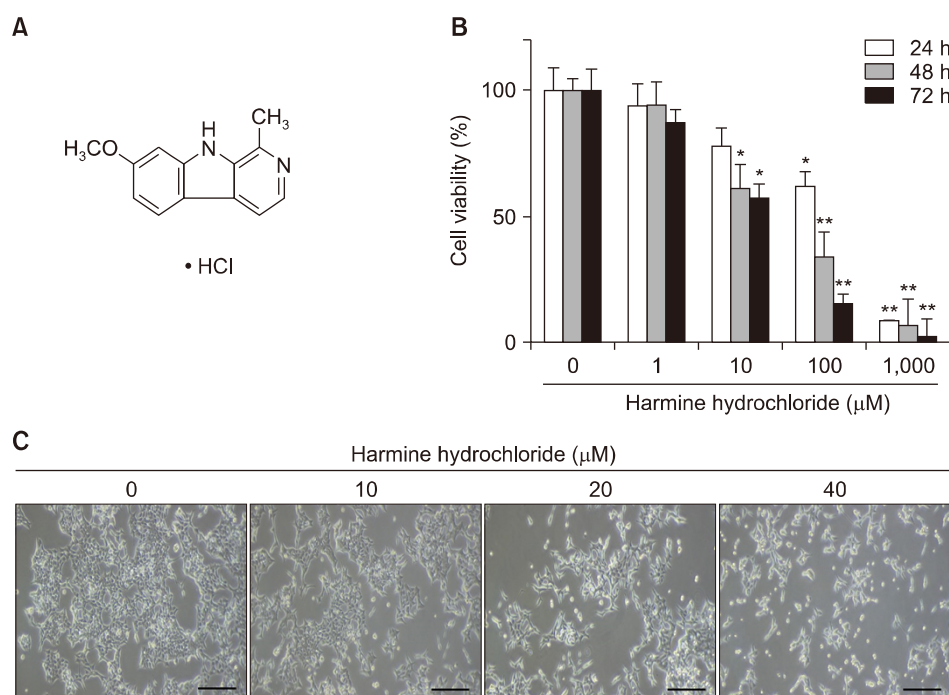


Fig. 1. Effect of harmine hydrochloride (HMH) on HCT116 cell growth. (A) Chemical structure of HMH. (B) Cell viability curve obtained with varying concentrations of HMH. Cells were treated with 0, 1, 10, 100, and 1,000 μM HMH for 24, 48, and 72 h, and cell viability was measured using MTT assays. Results are presented as mean \pm SD, and analyzed by Student's *t*-test (* $P < 0.05$ and ** $P < 0.01$ vs. the control group). (C) Morphological changes. HMH inhibited growth of HCT116 cells in a dose-dependent manner. Cell morphology was visualized by inverted microscopy ($\times 200$). Scale bar, 50 μm . MTT, 3-(4,5-dimethylthiazol-2-yl)-2,5-diphenyltetrazolium bromide.

placed with fresh RPMI-1640 medium supplemented with 0~1,000 μM HMH for 24~72 h. Following incubation, 20 μL of MTT (5 mg/mL) reagent was added to each well, and plates were incubated for 3~4 h. The medium was removed, and each well was treated with 100 μL of DMSO to stop the reactions. Optical density was measured at 570 nm using a Synergy HTX plate reader (BioTek Instruments Inc., Winooski, VT, USA), and the data were analyzed using Gen5 software (BioTek Instruments Inc.).

Wound healing assay for cell migration analysis

Approximately 5×10^5 cells were seeded into a six-well plates and incubated for 24 h. Cells were artificially wounded using a P20 pipette tip, the cell monolayer rinsed with fresh medium to remove dead cells, and cells were treated with 0~40 μM HMH in fresh medium containing 1% FBS for 24~72 h. Images were obtained using an inverted microscope equipped with a camera during the 24~72 h of incubation. Wound healing areas were measured using ImageJ software (National Institutes of Health, Bethesda, MD, USA).

Colony-formation assays

Cells were plated at a density of 1,000 cells/well in a six-well plates with 2 mL of RPMI-1640 medium containing 10% FBS. Cells were incubated for 24 h in RPMI-1640 medium containing varying concentrations of HMH at 37°C in a 5% CO₂ incubator, and the medium was replaced with fresh medium without HMH every 3~4 days. Colony formation was examined after 14 days of incubation. Then, colonies (>50 cells) were fixed in methanol for 15 min, stained with 0.1% crystal violet for 10 min, and counted under a microscope (FV500, Olympus, Tokyo, Japan).

Flow cytometry for cell cycle distribution analysis

Cells were seeded in 100-mm culture plates and incubated for 24 h. After ensuring that the cell density was $\geq 70\%$, cells were treated with 0~40 μM HMH for 48 h. Subsequently, cells were harvested with trypsin/ethylenediaminetetraacetic acid and fixed in 70% cold ethanol overnight. The fixed cells were centrifuged at 5,000 rpm at 4°C for 5 min, washed, and incubated with RNase A (50 $\mu\text{g}/\text{mL}$) at 37°C for 30 min for cell cycle analysis. Cells were stained with 50 $\mu\text{g}/\text{mL}$ propidium iodide (PI) at 37°C for 30 min, and the DNA content was analyzed using CellQuest and a FACS Vantage SE flow cytometer (BD Biosciences).

Cell apoptosis analysis

Cell apoptosis assays were performed using HCT116 cells treated with HMH for 48 h, according to the protocol

provided by the Annexin V-fluorescein isothiocyanate (FITC) apoptosis detection kit (BD Biosciences). Cells were prepared at a density of 1×10^5 cells/mL in binding buffer and incubated with Annexin V-FITC and PI in the dark for 30 min. The DNA content of the stained cells was analyzed using the CellQuest Software and a FACS Vantage SE flow cytometer (Becton Dickinson, Heidelberg, Germany).

Measurement of intracellular reactive oxygen species (ROS) accumulation

Intracellular ROS production was measured using the fluorescent dye (H₂DCFDA, Molecular Probe, Invitrogen). After treatment with 0~40 μM HMH for 48 h, cells were washed twice, stained with 20 μM H₂DCFDA for 30 min, and washed a further two times. H₂DCFDA reacts with ROS to form DCF, a fluorescent compound (Yoon et al., 2018). The amount of intracellular DCF was measured using flow cytometry (Becton Dickinson).

Determination of protein expression by Western blotting

Cells were treated with HMH (0, 10, 20, and 40 μM) for 48 h, then the proteins were extracted using PRO-PREP Protein Extraction Solution containing protease inhibitors and phosphatase inhibitors (Roche Diagnostics GmbH, Mannheim, Germany) at 4°C for 30 min. The extracted proteins were centrifuged at 4°C and 13,000 rpm for 30 min. Protein samples (40 μg) were then separated using 6%~12% sodium dodecyl sulfate polyacrylamide gel electrophoresis and transferred onto polyvinylidene fluoride membranes (Bio-Rad Laboratories Inc., Hercules, CA, USA). The membranes were blocked with 5% bovine serum albumin (BSA) (AMRESCO, Cleveland, OH, USA) prepared in Tris-buffered saline (TBS) with 0.1% Tween 20 (TBS-T) for 1 h and subsequently incubated with a primary antibodies (1:500~1:1,000) diluted with 5% BSA at 4°C overnight. Next, the membranes were washed four times (3 min each) with TBS-T. After washing, the membranes were incubated with HRP-conjugated anti-rabbit or anti-mouse secondary antibodies (1:1,000) for 1 h at room temperature, and reactions were detected using an Advanced Electrochemiluminescence Western Blot Detection Kit (Amersham, Uppsala, Sweden).

Statistical analyses

Data are presented as mean \pm SD for the indicated number of independent experiments. Statistical significance ($P < 0.05$) was determined using Student's *t*-test for paired data. Statistical analyses were performed using IBM SPSS for Windows (version 23.0; IBM Co., Armonk, NY, USA).

RESULTS

HMH inhibits growth of HCT116 cells

To investigate whether HMH effectively inhibits growth of human CRC cells, HCT116 cells were treated with HMH at varying concentrations (0~1,000 μM) for 24~72 h, and cell growth was examined. Following 24, 48, and 72 h of treatment, the IC_{50} values of HMH in HCT116 cells were 125.5, 58.2, and 37.8 μM , respectively (Fig. 1B). Cell growth was significantly inhibited after 24, 48, and 72 h of HMH treatment at concentrations ≥ 100 μM ($P < 0.05$ and $P < 0.01$, respectively). Based on these IC_{50} values, we examined morphological changes to HCT116 cells after treatment with HMH at concentrations of up to 40 μM to determine the concentration at which HMH induced low cytotoxicity and high biological activity (Fig. 1C).

HMH inhibits cell migration and colony formation

Scratches were created on 70%~80% confluent monolayers of HCT116 cells grown in culture dishes. FBS concentrations in the medium were reduced from 10% to 1%, and cell migration was examined after treatment with varying concentrations of HMH (0~40 μM) for 48 h. The wound healing area was 3.2% in the 40 μM HMH treatment group versus 63.1% in the control group, in-

dicating significant inhibition of cell migration after HMH treatment (Fig. 2A and 2C).

To investigate the inhibitory effect of HMH on colony formation, we treated HCT116 cells with varying concentrations of HMH for 24 h. The medium containing HMH was replaced with fresh medium without HMH, and the cells were cultured for a further 14 days. Colony formation was examined (Fig. 2B and 2D), and the number of colonies was observed to be significantly reduced by 95% in the group treated with 40 μM HMH compared to the control group ($P < 0.001$).

HMH induces G2/M cell cycle arrest and apoptosis

We examined the regulatory effect of HMH on HCT116 cell cycle progression because HMH was found to inhibit cell proliferation, migration, and colony formation in previous experiments. HCT116 cells were treated with HMH (0 to 40 μM) for 48 h, and the distribution of the cell cycle stages was examined. A dose-dependent reduction was observed in the distribution of cells in the G0/G1 phase. The proportion of cells in the G2/M phase was 61.61% in the 40 μM HMH treated group versus 13.71% in the control group (Fig. 3A and 3B). Western blotting was performed to examine the regulatory proteins in the G2/M phase. HMH increased expression of p53 and p21, which regulate the cell cycle, and reduced expression of

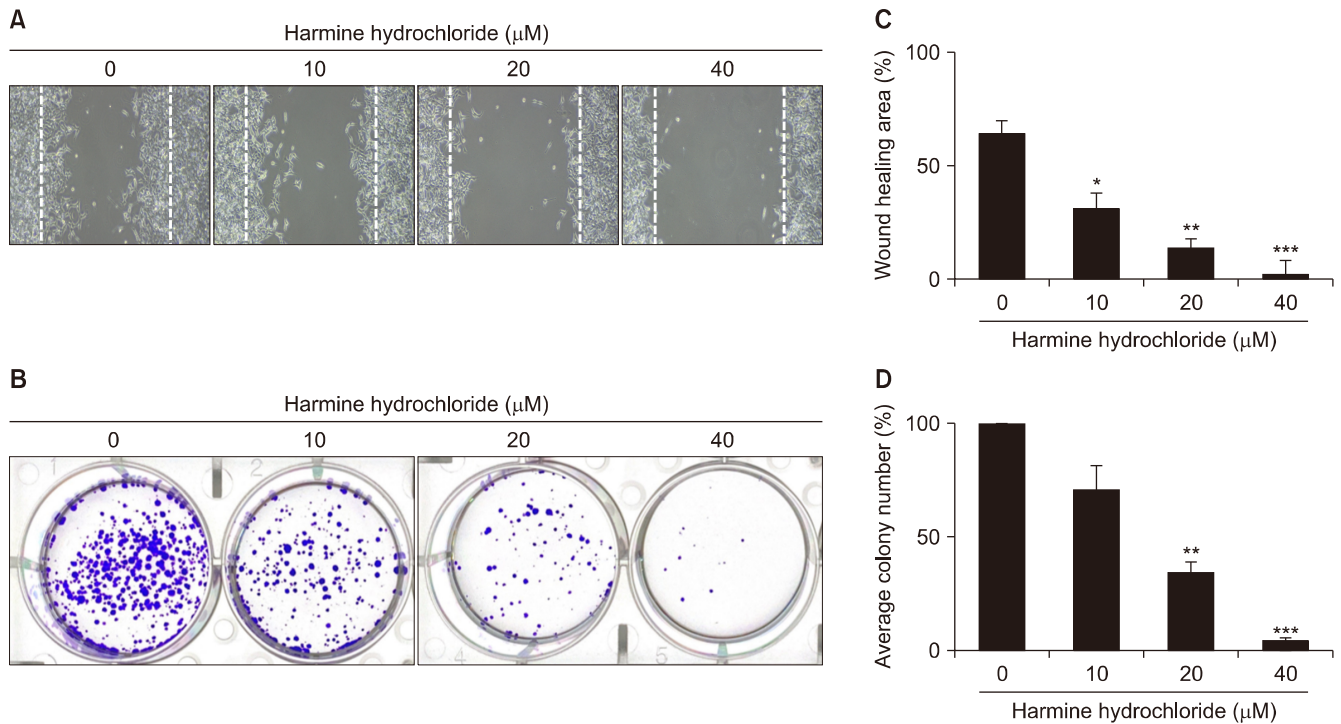


Fig. 2. Effect of harmine hydrochloride (HMH) on migration and the colony-formation ability of HCT116 cells. (A) Scratches were made to confluent cell monolayers in six-well plates, cells were treated with HMH (0~40 μM) for 48 h, and migration areas were measured. (B) Cells were seeded onto a six-well plate and treated with HMH at varying concentrations (0~40 μM) for 24 h. The medium was replaced with fresh medium every 3~4 days during a 14-day culture period. After examining colony formation, cells were fixed in methanol and stained with 0.5% crystal violet. (C and D) Cells were examined under a microscope, and wound areas and the number of colonies determined using ImageJ. Values are presented as mean \pm SD. * $P < 0.05$, ** $P < 0.01$, and *** $P < 0.001$ vs. control.

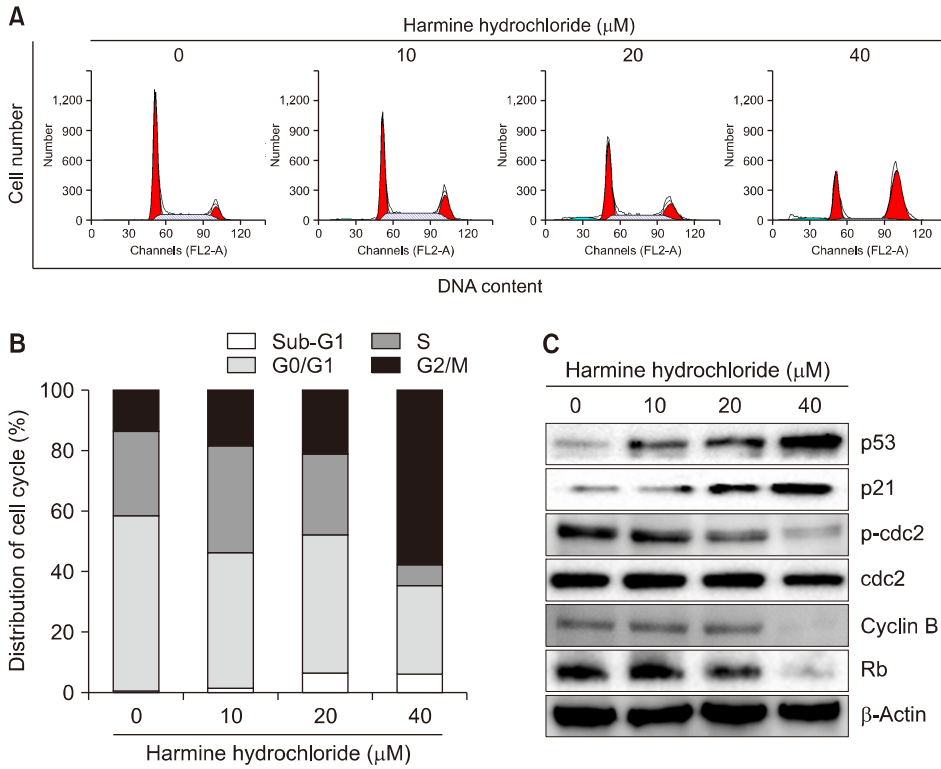


Fig. 3. Effect of harmine hydrochloride (HMH) on HCT116 cell cycle progression. (A) HCT116 cells were treated with HMH (0, 10, 20, and 40 μM) for 48 h and stained with propidium iodide. Flow cytometric analysis was performed to evaluate cell cycle progression. (B) Distribution of cells in the G0/G1, S, and G2/M phases following HMH treatment. HMH induced G2/M cell cycle arrest in a dose-dependent manner. (C) Western blotting was performed to examine expression of proteins associated with the G2/M phase, such as p53, p21, p-cdc2, cdc2, cyclin B, and Rb.

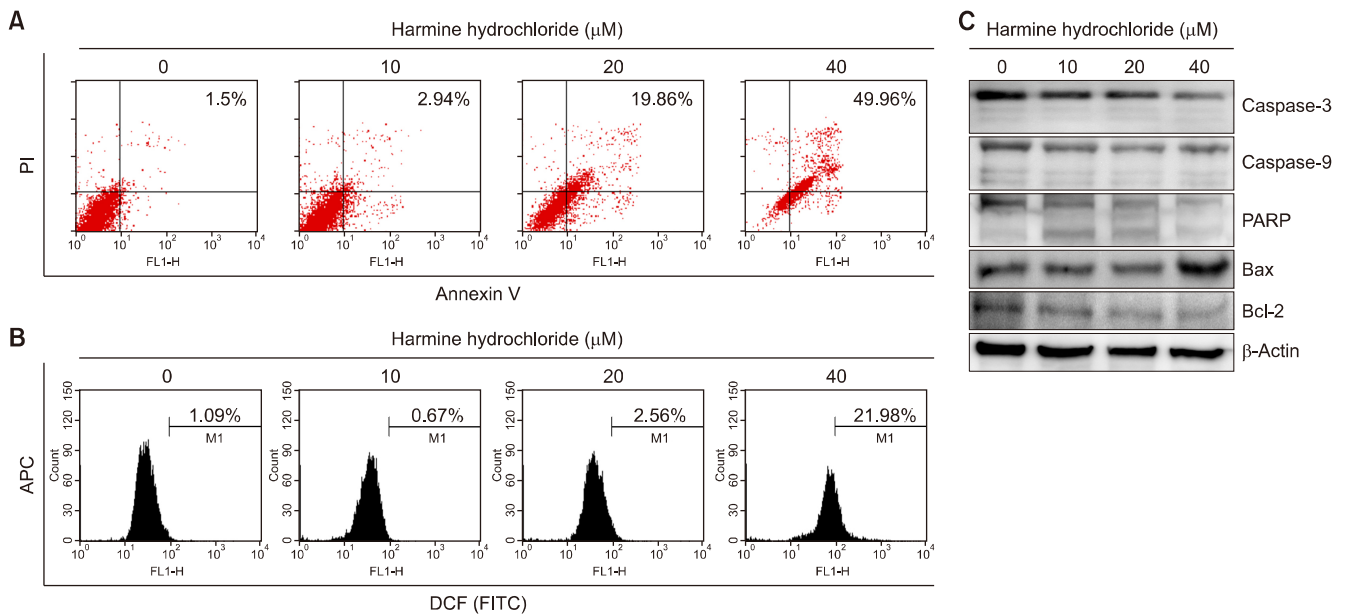


Fig. 4. Effect of harmine hydrochloride (HMH) on apoptosis and reactive oxygen species (ROS) production in HCT116 cells. (A) Cells were treated with HMH (0, 10, 20, and 40 μM) for 48 h, stained with Annexin V and propidium iodide (PI), and analyzed using a FACSCalibur flow cytometer. (B) ROS production was measured by dichlorofluorescein (DCF) quantification in HCT116 cells exposed to HMH (0~40 μM) for 48 h using H_2DCFDA . Data are the mean \pm SD in triplicate tests. (C) Western blotting was performed to determine the expression of pro-apoptotic and anti-apoptotic proteins in HCT116 cells treated with HMH. β -Actin was used as an internal control. APC, allophycocyanin; FITC, fluorescein isothiocyanate.

p-cdc2, cdc2, and cyclin B1, which regulate the G2/M phase, in a dose-dependent manner (Fig. 3C). Additionally, HMH reduced expression of Rb, a regulator of cell proliferation.

Because HMH was found to mediate cell cycle progression, we performed Annexin V-FITC/PI double staining to investigate whether HMH induces apoptosis. Treat-

ment with 20 and 40 μM HMH increased the apoptotic cell population by 19.86% and 49.96%, respectively (Fig. 4A). ROS production increased to 21.98% in the group treated with 40 μM HMH versus 1.09% in the control group (Fig. 4B). To investigate the mechanism underlying apoptosis, we performed Western blotting and examined the expression of apoptotic proteins such as caspase-3,

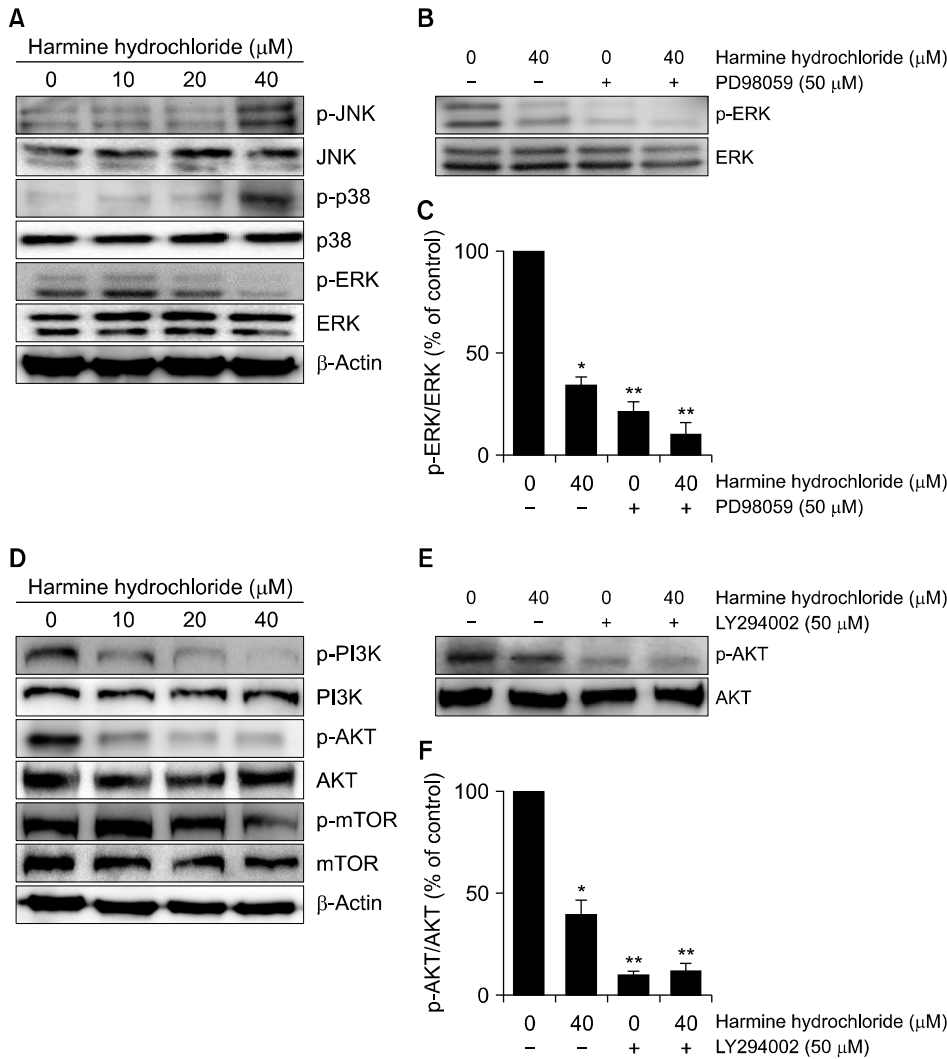


Fig. 5. Effect of harmine hydrochloride (HMH) on MAPK and PI3K/AKT/mTOR signaling pathways. Representative blots showing the expression of MAPKs (A) and proteins associated with the PI3K/AKT/mTOR pathways (D). HCT116 cells were treated with 0 or 40 μM HMH in combination with the ERK inhibitor PD98059 (B) or the AKT inhibitor LY294002 (E). Expression of p-ERK and p-AKT was examined by Western blotting. (C and F) Band intensity was normalized to total levels of ERK and AKT. Data are the mean \pm SD. * $P < 0.05$ and ** $P < 0.01$ compared with each total content.

caspase-9, and PARP; the pro-apoptotic protein Bax; and the anti-apoptotic protein Bcl-2 (Fig. 4C). HMH reduced expression of apoptotic proteins such as pro-caspase-3, pro-caspase-9, and PARP, and the anti-apoptotic protein Bcl-2 in a dose-dependent manner. In contrast, HMH increased expression of the pro-apoptotic protein Bax in a dose-dependent manner.

HMH regulates ERK and PI3K/AKT/mTOR signaling pathways

HMH increased expression of p-JNK and p-p38 and reduced expression level of p-ERK in a dose-dependent manner (Fig. 5A). Furthermore, p-ERK expression was significantly reduced in cells treated with the combination of PD98059 and HMH compared with control cells ($P < 0.05$ and $P < 0.01$, Fig. 5B and 5C). We investigated whether the PI3K/AKT/mTOR pathway was associated with the effect of HMH treatment on HCT116 cells (Fig. 5D). Western blotting was performed using proteins from HCT116 cells treated with 10, 20, and 40 μM HMH for 48 h to examine the inhibitory effect of HMH on protein expression. HMH reduced expression of p-PI3K, p-AKT,

and p-mTOR. In addition, in cells were treated with a combination of LY294002 and HMH (Fig. 5E and 5F), HMH significantly reduced the activity of p-AKT ($P < 0.05$ and $P < 0.01$). These results demonstrate that HMH inhibits cell proliferation and induces cell migration and apoptosis via ERK and PI3K/AKT/mTOR signaling pathways.

DISCUSSION

As interest in the development of novel natural product-derived pharmaceuticals with anticancer activity increases, studies have explored the anticancer activities of beta-carboline alkaloids, harmine, and harmine derivatives isolated from *P. harmala* L. seeds (Newman and Cragg, 2016). HMH has a similar structure to harmine, and both compounds possess identical pharmacological properties. HMH has excellent receptivity, and demonstrates anticancer activity against human gastric cancer cells and human hepatoma cells (Zhang et al., 2016; Tan et al., 2020). However, the mechanism of its anticancer activity toward CRC cells are unknown. In the present study, we dem-

onstrated that HMH reduces cell viability and induces G2/M arrest and apoptosis in HCT116 cells. Cell cycle progression is characteristic of all eukaryotic cells. The cell cycle has four major checkpoints: the G1/S, S, G2/M, and spindle assembly (Sánchez and Dynlacht, 2005). Cyclins and cyclin-dependent kinase (CDK) complexes play an important role in regulating different stages of cell cycle progression. The G1 and S2 phases are regulated by CDK2, CDK6, CDK4, cyclin D1 and cyclin E, the G2/M phase is regulated by CDK2, cdc2, cyclin A, and cyclin B, and G2/M transition is regulated by the cyclin B/cdc2 complex. A CDK inhibitor p21^{Waf1/Cip1} has been shown to inactivate the cyclin B1/cdc2 complex in p53-dependent sustained G2/M arrest (Smith et al., 2020). We showed that HMH induces G2/M cell cycle arrest, significantly upregulates p53 and p21 protein expression, and downregulates cyclin B1, p-cdc2, and cdc2 expression in HCT 116 cells.

Apoptosis is a type of programmed cell death that occurs under normal physiological or pathological conditions, and is induced via various pathways, including the death receptor and mitochondrial pathways, and during endoplasmic reticulum stress (Iurlaro and Muñoz-Pinedo, 2016). Various factors of the mitochondrial apoptosis pathway downregulate pro-survival proteins and upregulate pro-apoptotic proteins, reducing mitochondrial membrane potential and inducing cytochrome c release from mitochondria. Cytochrome c induces apoptosis within the cytoplasm by activating caspase-9 and caspase-3 and promoting PARP degradation (Gogvadze et al., 2009). Bcl-2 family proteins play an important role in regulating apoptosis (Zhou et al., 2011). Apoptosis occurs when expression of anti-apoptotic proteins in the mitochondrial membrane, such as Bcl-2 and Bcl-xL, decrease and the ratio of pro-apoptotic proteins such as Bax (Bcl-2/Bax, Bcl-xL/Bax) relatively reduce, increase, or remain unchanged. In the present study, flow cytometry analysis showed a dose-dependent increase in the proportion of apoptotic HCT116 cells. Western blotting results confirmed that HMH reduced expression of pro-caspase-3, pro-caspase-9, PARP, and Bcl-2 and increased expression of Bax, consequently inducing apoptosis.

ROS plays an important role in apoptosis. Cancer cells appear to have high levels of endogenous oxidative stress, and cancer cell growth can be inhibited by increasing ROS production (Chen et al., 2017). Under pathological conditions, excessive ROS damages DNA, proteins, mitochondria, and the endoplasmic reticulum, and induces cell cycle arrest and apoptosis (Simon et al., 2000). In our study, HMH increased ROS production in a dose-dependent manner.

JNK and p38 MAPK play important roles in the regulating apoptosis and autophagy (Brancho et al., 2005; Dha-

nasekaran and Reddy, 2008). Activated JNKs are translocated to the mitochondria, where they phosphorylate the anti-apoptotic proteins Bcl-2 and Bcl-xL, reduce expression of the isomers Bax, Bcl-2, or Bcl-xL, and separate Bax to induce cell apoptosis (Jeong et al., 2008). Activated EPKs induce apoptosis in response to a wide range of stimuli. Indeed, ERKs inhibit pro-apoptotic proteins such as caspase-8, caspase-9, Bad, Bim, and signal transducer and activator of transcription 3/5, and activate anti-apoptotic proteins such as Bcl-xL, c-Flip, immediate early response gene X-1, and cAMP-response element-binding protein through phosphorylation. Similar to AKTs, activated ERKs regulate many cellular events, including cell proliferation and survival (Peng et al., 2010; Samatar and Poulikakos, 2014). In this study, we found that HMH upregulates ERKs and downregulates proteins associated with cell cycle arrest and mitochondrial apoptosis. Western blotting results showed that HMH upregulates p-JNK and p-p38 expression and downregulates p-ERK expression in HCT116 cells; thus, HMH inhibites ERK expression and induced cell apoptosis.

AKT signaling induces cell proliferation and apoptosis, and regulates expression of apoptotic proteins, such as the Bcl-2 family proteins (Zhang et al., 2015). In this study, we demonstrated that inactivation or inhibition of the PI3K/AKT/mTOR pathway leads to downregulation of cyclin B1 and cdc2 expression and, subsequently, G2/M cell cycle arrest.

In the present study, HMH inhibited the growth of human CRC HCT116 cells by inducing cell cycle arrest and apoptosis, reduced the proportion of cells in the G0/G1 phase, and increased the proportion of cells in the G2/M phase. Additionally, HMH induced apoptosis by regulating expression of the Bcl-2 family genes and mitochondrial proteins and, in combination with ERK or AKT inhibitors, reduced p-ERK and p-AKT expression. These results demonstrated that ERK and PI3K/AKT/mTOR pathway inhibition may be involved in HMH-induced cell cycle arrest and apoptosis in HCT116 cells. The results of our study indicate the potential therapeutic application of HMH in CRC treatment.

ACKNOWLEDGEMENTS

This work was supported by National Research Foundation of Korea (NRF) grant funded by the Korea government (MSIT) (grant number 2020R1F1A1072191).

AUTHOR DISCLOSURE STATEMENT

The author declares no potential conflict of interest.

REFERENCES

- Arthur JS, Ley SC. Mitogen-activated protein kinases in innate immunity. *Nat Rev Immunol*. 2013. 13:679-692.
- Bahrami A, Khazaei M, Hasanzadeh M, ShahidSales S, Joudi Mashhad M, Farazestanian M, et al. Therapeutic potential of targeting PI3K/AKT pathway in treatment of colorectal cancer: rational and progress. *J Cell Biochem*. 2018. 119:2460-2469.
- Brancho D, Ventura JJ, Jaeschke A, Doran B, Flavell RA, Davis RJ. Role of MLK3 in the regulation of mitogen-activated protein kinase signaling cascades. *Mol Cell Biol*. 2005. 25:3670-3681.
- Chen X, Dai X, Zou P, Chen W, Rajamanickam V, Feng C, et al. Curcuminoid EF24 enhances the anti-tumour activity of Akt inhibitor MK-2206 through ROS-mediated endoplasmic reticulum stress and mitochondrial dysfunction in gastric cancer. *Br J Pharmacol*. 2017. 174:1131-1146.
- Das Thakur M, Stuart DD. Molecular pathways: response and resistance to BRAF and MEK inhibitors in BRAF(V600E) tumors. *Clin Cancer Res*. 2014. 20:1074-1080.
- Dhanasekaran DN, Reddy EP. JNK signaling in apoptosis. *Oncogene*. 2008. 27:6245-6251.
- Gogvadze V, Orrenius S, Zhivotovsky B. Mitochondria as targets for cancer chemotherapy. *Semin Cancer Biol*. 2009. 19:57-66.
- Golob-Schwarzl N, Krassnig S, Toeglhofer AM, Park YN, Gogg-Kamerer M, Vierlinger K, et al. New liver cancer biomarkers: PI3K/AKT/mTOR pathway members and eukaryotic translation initiation factors. *Eur J Cancer*. 2017. 83:56-70.
- Iurlaro R, Muñoz-Pinedo C. Cell death induced by endoplasmic reticulum stress. *FEBS J*. 2016. 283:2640-2652.
- Jeong HS, Choi HY, Choi TW, Kim BW, Kim JH, Lee ER, et al. Differential regulation of the antiapoptotic action of B-cell lymphoma 2 (Bcl-2) and B-cell lymphoma extra long (Bcl-xL) by c-Jun N-terminal protein kinase (JNK) 1-involved pathway in neuroglioma cells. *Biol Pharm Bull*. 2008. 31:1686-1690.
- Kang DW, Lee BH, Suh YA, Choi YS, Jang SJ, Kim YM, et al. Phospholipase D1 inhibition linked to upregulation of ICAT Blocks colorectal cancer growth hyperactivated by Wnt/ β -catenin and PI3K/Akt signaling. *Clin Cancer Res*. 2017. 23:7340-7350.
- Kuebler JP, Wieand HS, O'Connell MJ, Smith RE, Colangelo LH, Yothers G, et al. Oxaliplatin combined with weekly bolus fluorouracil and leucovorin as surgical adjuvant chemotherapy for stage II and III colon cancer: results from NSABP C-07. *J Clin Oncol*. 2007. 25:2198-2204.
- Liu H, Han D, Liu Y, Hou X, Wu J, Li H, et al. Harmine hydrochloride inhibits Akt phosphorylation and depletes the pool of cancer stem-like cells of glioblastoma. *J Neurooncol*. 2013. 112:39-48.
- McChesney JD. Natural products in drug discovery—organizing for success. *P R Health Sci J*. 2002. 21:91-95.
- Mukherjee AK, Basu S, Sarkar N, Ghosh AC. Advances in cancer therapy with plant based natural products. *Curr Med Chem*. 2001. 8:1467-1486.
- Murthy D, Attri KS, Singh PK. Phosphoinositide 3-kinase signaling pathway in pancreatic ductal adenocarcinoma progression, pathogenesis, and therapeutics. *Front Physiol*. 2018. 9:335. <https://doi.org/10.3389/fphys.2018.00335>
- Newman DJ, Cragg GM. Natural products as sources of new drugs from 1981 to 2014. *J Nat Prod*. 2016. 79:629-661.
- Papadatos-Pastos D, Rabbie R, Ross P, Sarker D. The role of the PI3K pathway in colorectal cancer. *Crit Rev Oncol Hematol*. 2015. 94:18-30.
- Peng S, Zhang Y, Zhang J, Wang H, Ren B. ERK in learning and memory: a review of recent research. *Int J Mol Sci*. 2010. 11:222-232.
- Peti W, Page R. Molecular basis of MAP kinase regulation. *Protein Sci*. 2013. 22:1698-1710.
- Qin H, Liu L, Sun S, Zhang D, Sheng J, Li B, et al. The impact of PI3K inhibitors on breast cancer cell and its tumor microenvironment. *PeerJ*. 2018. 6:e5092. <https://doi.org/10.7717/peerj.5092>
- Sabio G, Davis RJ. TNF and MAP kinase signalling pathways. *Semin Immunol*. 2014. 26:237-245.
- Samatar AA, Poulikakos PI. Targeting RAS-ERK signalling in cancer: promises and challenges. *Nat Rev Drug Discov*. 2014. 13:928-942.
- Sánchez I, Dynlacht BD. New insights into cyclins, CDKs, and cell cycle control. *Semin Cell Dev Biol*. 2005. 16:311-321.
- Simon HU, Haj-Yehia A, Levi-Schaffer F. Role of reactive oxygen species (ROS) in apoptosis induction. *Apoptosis*. 2000. 5:415-418.
- Smith HL, Southgate H, Tweddle DA, Curtin NJ. DNA damage checkpoint kinases in cancer. *Expert Rev Mol Med*. 2020. 22:e2. <https://doi.org/10.1017/erm.2020.3>
- Tan B, Li Y, Zhao Q, Fan L, Zhang M. The impact of harmine hydrochloride on growth, apoptosis and migration, invasion of gastric cancer cells. *Pathol Res Pract*. 2020. 216:152995. <https://doi.org/10.1016/j.prp.2020.152995>
- Torre LA, Bray F, Siegel RL, Ferlay J, Lortet-Tieulent J, Jemal A. Global cancer statistics, 2012. *CA Cancer J Clin*. 2015. 65:87-108.
- Turjanski AG, Vaqué JP, Gutkind JS. MAP kinases and the control of nuclear events. *Oncogene*. 2007. 26:3240-3253.
- Yoon DS, Lee MH, Cha DS. Measurement of intracellular ROS in *Caenorhabditis elegans* using 2',7'-dichlorodihydrofluorescein diacetate. *Bio Protoc*. 2018. 8:e2774. <https://doi.org/10.21769/BioProtoc.2774>
- Zhang J, Yu XH, Yan YG, Wang C, Wang WJ. PI3K/Akt signaling in osteosarcoma. *Clin Chim Acta*. 2015. 444:182-192.
- Zhang L, Li D, Yu S. Pharmacological effects of harmine and its derivatives: a review. *Arch Pharm Res*. 2020. 43:1259-1275.
- Zhang P, Huang CR, Wang W, Zhang XK, Chen JJ, Wang JJ, et al. Harmine hydrochloride triggers G2 phase arrest and apoptosis in MGC-803 cells and SMMC-7721 cells by upregulating p21, activating caspase-8/Bid, and downregulating ERK/Bad pathway. *Phytother Res*. 2016. 30:31-40.
- Zhou F, Yang Y, Xing D. Bcl-2 and Bcl-xL play important roles in the crosstalk between autophagy and apoptosis. *FEBS J*. 2011. 278:403-413.